

LENSING, REDDENING AND EXTINCTION EFFECTS OF MGII ABSORBERS FROM $Z = 0.4$ TO $Z = 2$

BRICE MÉNARD¹, DANIEL NESTOR², DAVID TURNSHEK³, ANNA QUIDER³,
GORDON RICHARDS⁴, DORON CHELOUCHE⁵ & SANDHYA RAO³

Draft version August 27, 2018

Abstract

Using a sample of almost 7000 strong MgII absorbers with $0.4 < z < 2.2$ detected in the SDSS DR4 dataset, we investigate the gravitational lensing and dust extinction effects they induce on background quasars. After carefully quantifying several selection biases, we isolate the reddening effects as a function of redshift and absorber rest equivalent width, W_0 . We find the amount of dust to increase with cosmic time as $\tau(z) \propto (1+z)^{-1.1 \pm 0.4}$, following the evolution of cosmic star density or integrated star formation rate. We measure the reddening effects over a factor 30 in E(B–V) and we find that $\tau \propto (W_0)^{1.9 \pm 0.1}$, providing us with an important scaling for theoretical modeling of metal absorbers. We also measure the dust-to-metals ratio and find it similar to that of the Milky Way. In contrast to previous studies, we do not detect any gravitational magnification by MgII systems. We measure the upper limit $\mu < 1.10$ and discuss the origin of the discrepancy. Finally, we estimate the fraction of absorbers missed due to extinction effects and show that it rises from 1 to 50% in the range $1 < W_0 < 6 \text{ \AA}$. We parametrize this effect and provide a correction for recovering the intrinsic $\partial N / \partial W_0$ distribution.

Subject headings: quasars – absorbers: MgII – gravitational lensing: statistical – reddening – dust

1. INTRODUCTION

Quasar absorption lines provide us with a unique tool to probe the gas content in the Universe. They offer an unmatched sensitivity up to high redshift, allow us to detect arbitrarily faint objects, and constrain the gas distribution in velocity space. However, the lack of direct spatial information tends to be a limitation for understanding the nature of these systems and fundamental questions still remain. One way to overcome this problem is to relate the gas distribution to that of other components such as dark matter, stars and dust by measuring their cross-correlations.

Galactic environments have been studied using various types of absorption lines. Among metal lines, the MgII doublet, $\lambda\lambda 2796, 2803 \text{ \AA}$, has been extensively used due to the strength and wavelength of the transitions making it easily detectable from the ground at $0.4 \lesssim z \lesssim 2.2$ (Lanzetta et al. (1987); Steidel & Sargent (1992); Nestor et al. (2005); Prochter et al. (2006)). MgII turns out to be a sensitive tracer of galactic environment: it arises in gas spanning more than five decades of neutral hydrogen column density (e.g. Churchill et al. 2000), and it has been shown that the detection of a strong MgII absorber indicates the presence of a nearby $\sim 0.1 - 10 L_*$ galaxy along the line-of-sight (Bergeron & Boissé 1991; Steidel et al. 1994; Bergeron et al. 1992; Le Brun et al. 1993; Steidel et al. 1994, 1997), and at low redshift

Rao et al. (2006) have shown that strong MgII absorbers are good tracers of Damped Lyman alpha systems. For reviews of the progress on the determination of these systems, see Tripp & Bowen (2005) and Churchill et al. (2005).

Recently, the size and homogeneity the SDSS has allowed several statistical analyzes to be done: Bouché et al. (2006) measured the cross-correlation between $z \sim 0.5$ luminous red galaxies and MgII absorbers. Zibetti et al. (2005, 2007) investigated the distribution of absorber impact parameters and the emission properties of MgII related galaxies. They have shown that a cross-correlation between light and gas can be detected up to 200 kpc and that stronger absorbers are related to bluer galaxies. The SDSS has also provided us with closely separated quasar pairs allowing us to analyze the spectrum of background quasars to probe the gas distribution around foreground ones (Bowen et al. 2006, 2007). Such a technique allows us to compare the gaseous halos of quasars and galaxies and it can ultimately be used to test the quasar unification scheme on large scales (Chelouche et al. 2007).

However, despite significant observational progress fundamental questions such as the nature of the gas seen in absorption and its spatial distribution still remain. More importantly, we still do not understand the process(es) responsible for the observed values of MgII rest equivalent widths. As strong MgII absorbers are known to be tracers of galaxies, they are expected to induce gravitational lensing and reddening effects to the light of their background quasars. Correlations between quasar magnitudes and the presence or strength of metal lines can therefore be used in order to quantify the relationships between gas, dark matter and dust. Such an approach also allows us to quantify the extinction and magnification biases in samples of optically selected quasars.

¹ Canadian Institute for Theoretical Astrophysics, University of Toronto, 50 St George street, Toronto ON

² Institute of Astronomy, University of Cambridge, Madingley Road, Cambridge. CB3 0HA, U.K.

³ Dept. of Physics and Astronomy, University of Pittsburgh, Pittsburgh, PA 15260, USA

⁴ Department of Physics, Drexel University, 3141 Chestnut Street, Philadelphia, PA 19104.

⁵ Institute for Advanced Study, Einstein Drive, Princeton NJ 08540, USA

1.1. Dust reddening

The presence of dust associated with various types of absorbers has been reported by many authors: Pei et al. (1991) & Pei (1992) found quasars with DLAs to be on average redder than quasars without. Richards et al. (2001) observed a similar effect with CIV absorption lines. Using the 2dF survey Ménard & Péroux (2003) found evidence of reddening due to strong MgII systems. Hopkins et al. (2004) showed that a fraction of SDSS quasars are reddened with SMC-type dust and argued that this effect comes predominantly from dust located at the quasar redshifts. Using the SDSS database, Wild & Hewett (2005); Wild et al. (2006) found an $E(B-V) \simeq 0.06$ associated with CaII absorbers, and York et al. (2006) & Khare et al. (2005) measured the mean reddening effects of about 800 quasars with $z > 1$ MgII absorbers. Constraints on dust can also be obtained by measuring the relative abundances of volatile and refractory elements in order to infer a depletion level (e.g. Vladilo & Péroux 2005; Vladilo et al. 2006; Nestor et al. 2003).

While the presence of dust reddening associated with metal absorbers has been convincingly shown, its detailed properties (dependencies on redshift, rest equivalent width, etc.) need to be quantified in order to understand the underlying physics and connect theory to observations.

The presence of dust along given lines-of-sight also implies the existence of a dust obscuration bias that can affect quasar and absorber number counts. Using 75 radio-selected quasars, Ellison et al. (2004) investigated such an effect and did not find any difference (at the 20% level) between the incidence of MgII absorbers in radio-selected and optically-selected quasars. This result shows that *in general* optically-selected quasars are not strongly affected by an extinction bias, but it does not provide us with the full information: it does not show how the shape of the observed distribution of absorber rest equivalent widths is affected by dust extinction.

In order to unveil the relationships between extinction and absorption properties, we present a new analysis based on the Sloan Digital Sky Survey (SDSS, York et al. 2000) using the fourth data release (DR4). After having quantified the efficiency of the SDSS pipeline to detect reddened quasars, we use a sample of about 7,000 MgII absorbers – i.e. almost an order of magnitude larger than previous studies – to measure the excess reddening induced by these systems and investigate its dependence on absorption rest equivalent width and redshift.

1.2. Gravitational lensing

In addition to cause reddening effects, the presence of a galaxy along the line-of-sight is expected to give rise to gravitational lensing effects. Several cases of strong gravitational lensing of quasars due to an absorbing galaxy are known (e.g. Turnshek et al. 1997). However, in general, the impact parameters of MgII absorbers are larger than a few kpc and gravitational lensing effects occur in the weak regime and solely change quasar magnitudes (Bartelmann & Loeb 1996; Perna et al. 1997; Smette et al. 1997; Bartelmann & Loeb 1998; Ménard 2005). The detection of such an effect would ultimately allow us to constrain the mass of MgII systems.

Several authors have attempted to detect the statistical magnification induced by MgII systems. Some have looked for redshift distribution changes (Thomas & Webster 1990; Borgeest & Mehlert 1993) but did not find any compelling evidence for gravitational lensing. Others have investigated the occurrence of metal absorbers (CIV, SiIV, MgII) on bright and faint quasars (York et al. 1991; Vanden Berk et al. 1996; Richards et al. 1999) and reported possible magnification effects for certain absorber species only. Ménard & Péroux (2003) used the 2dF-Quasar survey to compare the number of quasars with and without MgII absorbers as a function of magnitude and reported a relative excess of optically bright radio-selected quasars with absorbers as well as indications of reddening effects. Murphy & Liske (2004) applied the same method to a sample of Damped Lyman- α systems and reported a similar trend found at 2σ . Using radio-selected quasars, Ellison et al. (2004) reported a possible excess of optically bright quasars with MgII absorbers, and more recently Prochaska et al. (2005) found that quasars with high-redshift DLAs are on average brighter than quasars without. The various results found among all these analyzes turn out to be rather difficult to combine because the absorber species, redshift and equivalent width ranges differ. In addition, as noted in some of these analyzes, biases due to selection effects can mimic the lensing signal: it is easier to detect absorption lines in high quality (or high S/N) spectra, however, these spectra tend to correspond to bright objects. This selection bias results in a preference for detecting absorption lines in brighter quasars, which is an effect similar to the signal of interest. Unfortunately, none of these works could convincingly demonstrate that the level of such systematics was sufficiently low in their analysis, leaving the amplitude of lensing effects rather uncertain.

In this paper we attempt to make a significant improvement in making such a measurement by overcoming the problem of systematic effects using Monte Carlo simulations and by reaching a much higher precision thanks to the size and homogeneity of the SDSS. We use a robust semi-automatic absorption line finder algorithm, carefully select a population of reference quasars, test potential biases, and use Monte Carlo simulations to measure and quantify the level of systematics of our selection procedure. To detect a magnification signal we will apply the method proposed by Ménard (2005) and look for a correlation between the presence of absorbers and a change in the mean magnitude of their background quasars. Contrarily to previous studies, this approach allows the use of a non-parametric estimator.

The outline of the paper is as follows: in §2 we introduce the formalism of dust extinction and gravitational magnification. We describe the data used in our analysis in §3 as well as the selection of the different samples of quasars. The magnitude shifts and color changes due to the presence of absorbers along quasar lines-of-sight are presented in §4. We discuss the results and conclude in §5.

2. FORMALISM

Strong MgII absorbers (usually defined with $W_0(2796) > 0.3 \text{ \AA}$) are known to be tracers of galaxies

with luminosities ranging from 0.1 to several L_* . The presence of such a system seen along the line-of-sight of a background source can therefore modify its brightness in two ways: first, the presence of dust in and/or around the absorber can extinct and redden the source's light and second, it can act as a gravitational lens and amplify the flux of the source. This can be described by

$$f(\lambda) = f_{\text{ref}}(\lambda) \mu e^{-\tau_\lambda}, \quad (1)$$

where $f(\lambda)$ is the observed flux of a source behind an absorber, $f_{\text{ref}}(\lambda)$ is the flux that would be observed without intervening system, τ_λ is the optical depth for extinction induced by the galaxy and μ the gravitational amplification. The corresponding magnitude change can then be written

$$\begin{aligned} \delta m &= m - m_{\text{ref}} \\ &= -2.5 \log(\mu) + \frac{2.5}{\ln 10} \tau_\lambda. \end{aligned} \quad (2)$$

These two contributions have different wavelength and redshift contributions. One can therefore attempt to constrain them separately.

2.1. Measuring reddening effects

Following Ménard (2005), we introduce the observed mean magnitude difference between a population of quasars with absorbers and one without:

$$\Delta \langle m_j \rangle = \langle m_j \rangle - \langle m_{j,\text{ref}} \rangle, \quad (3)$$

where m_j is the magnitude in a given band j . In the next section we will measure this quantity using a large sample of MgII absorbers from the SDSS. We will then investigate how $\Delta \langle m_j \rangle$ varies as a function of absorber rest equivalent width and redshift. Similarly, we can then define the mean excess color

$$\langle E(j - k) \rangle = \Delta \langle m_j \rangle - \Delta \langle m_k \rangle \quad (4)$$

where j and k denote two different bands. It should be noted that such a quantity is not sensitive to gravitational lensing effects as it no longer depends on the magnification μ . It can be used to probe the statistical properties of the extinction curve of absorbers systems as well as the dust column densities as a function of absorber rest equivalent width.

In optical surveys, sources like quasars are both magnitude and color selected. When dust extinction occurs, such sources can become undetectable because they become too faint and/or too red. As long as sources are no longer detectable because of a limiting magnitude and not because of a color cut, we have

$$\langle E(j - k) \rangle = \frac{2.5}{\ln 10} \langle \tau(\lambda_j) - \tau(\lambda_k) \rangle. \quad (5)$$

However, if the sources become undetectable because they no longer satisfy a color cut, the measured reddening is then lower than the intrinsic one. Such a property depends on the details of the quasar selection procedure and will be addressed in section 3.2.

The current study is based on the photometry of SDSS quasars using the u, g, r, i, z filter set. However, historically people have quantified color excesses using the

Johnson B and V filters. In order to be able to present our results in similar units, we provide here a list of useful conversions. First, it should be noted that previous statistical studies (Khare et al. 2005; Ménard et al. 2005; York et al. 2006; Wild et al. 2006) have indicated that, on average, the extinction curves of MgII selected galaxies are consistent with that of the SMC, i.e. do not present an excess around the rest frame wavelength of $0.2 \mu\text{m}$ (in the optical, such a feature can only be detected for systems at redshift greater than ~ 1 and is therefore irrelevant for lower redshift galaxies). In this paper we will therefore consider only SMC-type extinction curves. We will also see in section §4 that such a property is confirmed by the present analysis.

In the range 0.1 to $1 \mu\text{m}$, the SMC extinction curve⁶ can be very well approximated by a power law $A_V \propto \lambda^{-1.2}$ (Prevot et al. 1984). By using the g and i filters, the conversion between the two color systems therefore reads

$$\begin{aligned} E(g - i) &= \frac{\lambda_g^{-1.2} - \lambda_i^{-1.2}}{\lambda_B^{-1.2} - \lambda_V^{-1.2}} \times E(B - V) \\ &\simeq 1.55 \times E(B - V) \end{aligned} \quad (6)$$

and the average wavelengths for a flat spectrum are given by $\{\lambda_g, \lambda_i, \lambda_B, \lambda_V\} = \{468, 748, 435, 555\}$ nm. Using the effective wavelength for realistic quasar spectra does not change the results significantly. In practice, two frames are interesting for considering colors excesses: in order to quantify the fraction of sources missed because of an extinction bias, *observed* $E(B-V)$ values are relevant. However, for estimating the amount of dust associated with an absorber system the *rest frame* $E(B-V)$ is the quantity of interest. For an SMC-like extinction curve we have

$$E(B - V)_{\text{obs}} = E(B - V)_{\text{rest}} (1 + z)^{1.2}. \quad (7)$$

In a given band, we will therefore observe almost four times more extinction by an absorber at $z = 2$ than the same system located at $z = 0$. For an SMC extinction curve we also have $A_v \simeq C_A \times E(B - V)$ where the proportionality coefficient C_A depends on the redshift of the dust and varies from 3.2 to 2.0 when z is in the range 0.5 to 2.0, with a mean value of 2.6.

2.2. Measuring gravitational lensing effects

In this section we show how magnification effects can (or cannot) affect the observed magnitude of distant sources like quasars. For more details we refer the reader to the original discussion presented in Ménard (2005).

Here we will first assume that extinction effects can be neglected (which is expected at sufficiently large wavelengths). Let us consider an area of the sky which is large enough for the mean magnification to be close to unity. In this area, let us consider a population of sources, with a fraction f of them lying behind an absorber system. We will write the magnitude distribution of the sources behind absorbers $N(m)$, and $N_{\text{ref}}(m)$ for the non-absorbed sources. We then have the following relation between the magnitude number counts:

$$N(m) = f \times \int N_{\text{ref}}(m - \delta m) P(\delta m) (\delta m), \quad (8)$$

⁶ Templates of the reddening curves can be obtained from <http://www.astro.princeton.edu/~draine>

where δm is the induced magnitude shift and $P(\delta m)$ is the probability density to have a given value of δm along a quasar line-of-sight. Note that in the case of absorber systems, f is not known. Observational estimates of the number density of absorbers are necessarily affected by lensing and/or extinction effects due to the need of background quasars to observe absorber systems. Therefore the only usable information from the previous equation comes from the shape of the distribution $N(m)$, i.e. its moments. In this paper we will focus only on the first moment, i.e. we will attempt to constrain the mean magnification and extinction effects by measuring the mean magnitude shift induced by the presence of absorber systems.

By defining $\langle m \rangle$ and $\langle m \rangle_{ref}$ to be the observed mean magnitudes of the two quasar populations, we see that the *observable* mean magnitude shift $\langle \Delta m_{obs} \rangle$ (eq. 3) can be used to probe the unknown distribution $P(\delta m)$. It is important to note that the *observed*-magnitude changes $\langle \Delta m_{obs} \rangle$ depend on both the magnification effects *and* the slope of the source luminosity distribution:

$$\langle \Delta m_{obs} \rangle = F[N(m)] \times \delta m, \quad (9)$$

and in general we have $\langle \Delta m_{obs} \rangle < \langle \delta m \rangle$. For SDSS quasars with $i < 20$, Ménard (2005) has shown that we have $\langle \Delta m_{obs} \rangle \simeq 0.30 \delta m$ where δm is an achromatic magnitude change. For a limiting magnitude of $i = 19.1$, we find $\langle \Delta m_{obs} \rangle \simeq 0.25 \delta m$.

It should be noted that if the number of sources as a function of luminosity follows a power law then $F = 0$ and magnitude changes cannot be observed whatever the value of the induced magnitude shift δm . This absence of observable lensing effects can be understood in the following way: gravitational magnification makes each source brighter but allows also new sources to be detectable as they become brighter than the limiting magnitude of a given survey. This latter effect increases the number of faint sources and tends to diminish the mean flux of the detected objects. For a power law luminosity distribution, the flux increase due to magnification is exactly canceled by the additional faint sources that enter the sample due to magnification, and lensing effects due to absorbers cannot be observed. Therefore, it is possible to detect changes in the magnitude distribution of a population lensed by absorbers only if its unlensed number counts depart from a power law as a function of luminosity. Extinction effects will be affected in a similar way but the ability to observe sources in different bands allows us to measure reddening effects and then infer the related extinction.

3. DATA & SELECTION BIASES

3.1. The quasar sample

In order to isolate the magnitude changes due to the presence of intervening absorber systems we need to compare the magnitude of quasars with absorption lines to that of a reference quasar population. Defining such a reference population without introducing any selection bias is a difficult task. Indeed, the detection of absorption lines depends on quasar redshift, spectrum S/N, and the extinction and reddening effects they might induce on their background source. All these effects have to be taken into account in order to carefully select a popula-

tion of reference quasars.

The first requirement is to work with a well defined sample of quasars. Among the large sample of quasars available from the SDSS DR4 sample ($N \sim 50,000$), we will use the primary spectroscopic quasar sample, i.e. quasars with $i < 19.1$ ($N \sim 29,000$), as the selection of these objects is based on a well defined series of color cuts (Schneider et al. 2002). We will not make use of fainter quasars (observed with SDSS serendipity fibers) as they are not selected from well defined selection criteria. Before characterizing the absorber systems used in this study, the first step of our analysis will be to investigate the sensitivity of the SDSS quasar target algorithm to reddening and extinction.

3.2. Detection of reddened quasars

Evidence for the presence of dust associated with MgII absorbers has already been shown by several authors by isolating the reddening and extinction effects they induce. Since the selection of quasars depends on quasar magnitudes and colors (Schneider et al. 2002), such an effect might introduce a bias in the object selection and it is therefore important to quantify it. In this section we now investigate the sensitivity of the SDSS quasar target algorithm (Richards et al. 2002) to reddening and extinction (similarly to the analysis done by Richards et al. 2003). In order to do so we use Montecarlo-like simulations to test the ability of the SDSS quasar algorithm to detect quasars for different amounts of reddening and extinction. We proceed as follows:

1. We use a sample of quasars without strong MgII absorber (as described in section 3.4), consider the SMC extinction curve and apply various amounts of extinction. We quantify the amount of reddening with the $E(B - V)$ excess.
2. The applied extinction will cause some objects to drop out of the input quasar sample as they become too faint and/or their colors no longer satisfy the series of selection criteria of the SDSS quasar selection algorithm, considering only non-radio and point sources. We reject the objects no longer labeled as quasars by the SDSS pipeline.
3. For each value of $E(B - V)$ applied, we measure the fraction of quasars missed due to limiting magnitude and color cuts effects, we measure the mean u, g, r, i and z magnitudes of the re-observed quasars and compare them to those of the initial sample of unreddened quasars.

We illustrate some of the results of this procedure in Fig. 1. From top to bottom we show the ability of the SDSS quasar selection algorithm to select quasars with increasing reddening and show the effects on quasar magnitudes. In each case we present the u, g, r, i and z -band magnitude distributions of the original (solid line histograms) and reddened samples (filled histograms). These panels show that the fraction of quasars missed due to dust extinction becomes substantial for observed reddening values of $E(B - V)$ larger than 0.2. In this figure we also show the mean magnitude of each sample with a vertical line. As the amount of extinction increases, we can easily observe reddening effects rising as

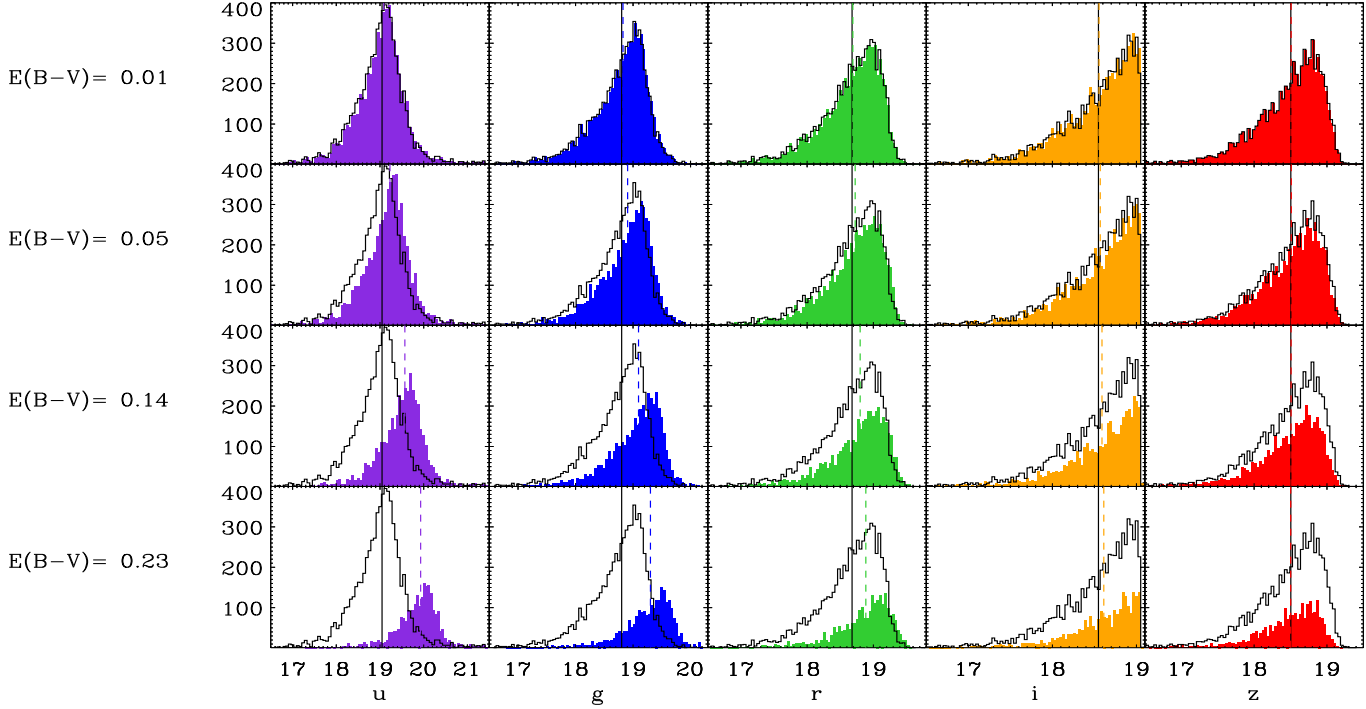


FIG. 1.— SDSS quasar detection sensitivity as a function of reddening. The solid-line histograms show the magnitude distribution of SDSS quasars without strong MgII absorber. The filled histograms show the fraction of objects that remain detectable after reddening effects. The vertical lines show the mean magnitude of each sample.

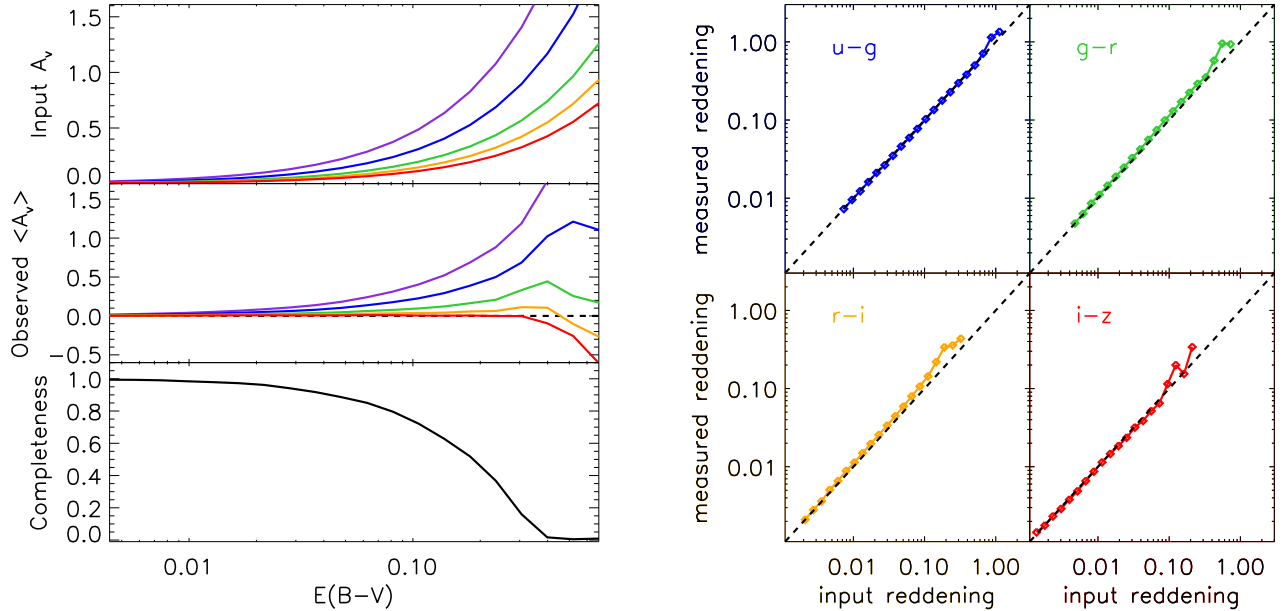


FIG. 2.— (Left) Top panel: amount of extinction as a function of $E(B-V)$ for an SMC reddening curve. Middle panel: measured mean magnitude shift of the detected objects. We observe that the measured extinction is lower than the initially induced one. Note that the mean z band magnitudes are not significantly affected by extinction. Lower panel: fraction of SDSS quasars still detectable after having applied a given extinction. Similarly to the analysis done by Richards et al. (2003), the SDSS quasar algorithm is able to recover most quasars reddened by $E(B-B) < 0.1$.

FIG. 3.— (Right) Measured reddening as a function of induced reddening. Even if the measured extinction differs from the induced ones, the color changes are not affected by the corresponding selection effects and in the reddening range of interest for the present study, the observed color changes of quasars can directly be used in order to quantify the amount of induced reddening by intervening absorbers.

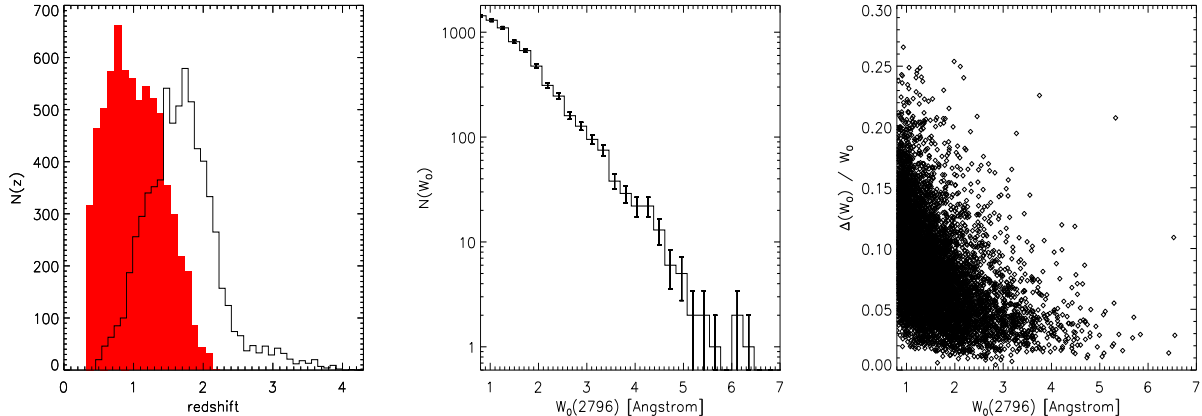


FIG. 4.— *left panel*: redshift distributions of detected MgII absorbers with $W_0 > 0.8 \text{ \AA}$ (filled histogram) and their background quasars (solid line). *Middle panel*: rest equivalent width distribution of the MgII systems detected in SDSS quasar, *right panel*: observed distribution of relative rest equivalent width uncertainty.

the mean magnitude shifts are more pronounced in bluer bands. In addition, we can observe that the mean magnitude in the z band is almost unaffected by reddening in the range considered here.

We present the summary of the completeness and reddening results in Figure 2. From top to bottom we show, as a function of $E(B-V)$, the input extinction, the measured extinction and the fraction of objects that can be detected. These results show that the observed extinction, defined as the difference between the mean magnitude of the reddened quasars and those of the initial sample, is always smaller than the induced extinction. As explained in section 4.1.5, such an effect is expected and is due to the shape of the quasar luminosity function. Moreover, we can see that the observed mean z -band magnitude is not significantly affected by extinction effects (for the range of reddening values of interest in this analysis). This property allows us to use the z band to constrain gravitational lensing effects. The bottom panel of the figure allows us to quantify the fraction of objects missed as a function of observed $E(B-V)$. By knowing the amount of reddening induced by a class of absorber systems one can use this curve to infer the fraction of objects missed by the SDSS quasar finder.

In the right panel of Figure 2, we show another property related to the selection of reddened quasars: the induced and measured *colors* are the same in the range of reddening values of interest in our case, i.e. with $E(B-V) < 0.5$. This indicates that the fraction of quasars lost due to color cuts is small. This property therefore allows us to measure the mean color excess of a sample of quasars and use the corresponding color value to infer the induced extinction.

The properties and selection biases of the SDSS target quasar algorithm will be used below to interpret the measurements. Our analysis is restricted to the main sample of SDSS spectroscopic quasars (with $i < 19.1$) in order to quantify certain selection effects. Including fainter quasars is expected to change the above numbers by a modest amount as the slope of quasar number counts distribution is a slowly varying function of mag-

nitude (see Richards et al. (2005)). Redshift-dependent selection effects are not considered here. As shown by Richards et al. (2002), the SDSS quasar selection algorithm is less efficient in detecting reddened quasars at $z \simeq 2.2$. This effect can be neglected in the present analysis as only a small fraction of objects are found at such a redshift (see Fig. 4).

3.3. Absorber systems

3.3.1. The MgII absorber sample

In order to investigate the effects of reddening and magnification due to intervening absorbers, we use the sample of MgII systems compiled with the method presented in Nestor et al. (2005) and based on SDSS DR4 data. In this section we briefly summarize the main steps involved in the absorption line detection procedure. For more details we refer the reader to Nestor et al. (2005).

All quasar spectra from the SDSS DR4 database were analyzed, regardless of QSO magnitude. The continuum-normalized SDSS QSO spectra were searched for MgII $\lambda\lambda 2796, 2803$ doublets using an optimal extraction method employing a Gaussian line-profile to measure each rest equivalent width W_0 . All candidates were interactively checked for false detections, a satisfactory continuum fit, blends with absorption lines from other systems, and special cases. The identification of Mg II doublets required the detection of the 2796 line and at least one additional line, the most convenient being the 2803 doublet partner. A 5σ significance level was required for all $\lambda 2796$ lines, as well as a 3σ significance level for the corresponding $\lambda 2803$ lines. Only systems $0.1c$ blue-ward of the quasar redshift and red-ward of Ly- α emission were accepted. For simplicity, systems with separations of less than 500 km/s were considered as a single system. The line finder is able to detect MgII absorption lines with a rest equivalent width $W_0 > 0.3 \text{ \AA}$. However a high completeness is reached only in the range $W_0 > 0.8 \text{ \AA}$. We will therefore focus our analysis on these stronger systems only. In such a range, multiple absorbers detected in the same quasar spectrum are found only in $\sim 15\%$ of the systems. For such cases we consider

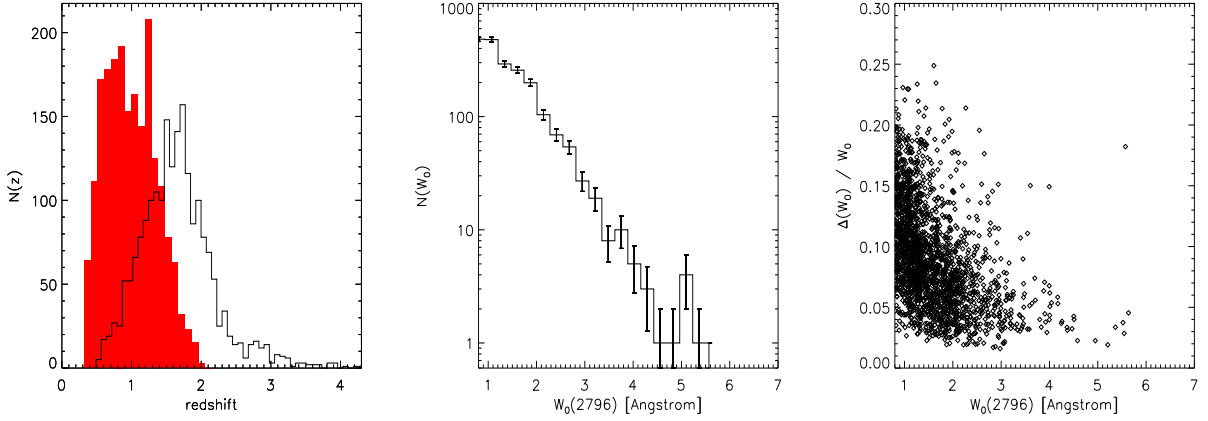


FIG. 5.— Properties of the simulated absorbers (see figure 4 for more information).

only the stronger system. We note that MgII absorption lines are in general saturated and in these cases no column density information can be directly extracted from $W_0^{\lambda 2796}$. The redshift distribution of the systems used in this analysis is presented in Figure 4. The filled histogram shows that of the MgII systems and the solid line their background quasars. The middle panel of Figure 4 shows the *observed* distributions of absorber rest equivalent width W_0 . The intrinsic distribution, i.e. corrected for incompleteness is presented in Nestor et al. (2005). The right panel of the figure shows the distribution of rest equivalent width measurement uncertainty. It shows the existence of a correlation between line detectability and absorber rest equivalent width. As can be seen, the relative W_0 uncertainty becomes larger for weaker systems. Because we require the 2796 Å absorption lines to be detected at least at the 5-sigma level, this results in a selection bias: weaker lines are preferentially found in high S/N spectra. In addition, given the fact that all SDSS quasars are taken with a similar exposure time, the selection criteria introduce a correlation between quasar brightness and spectrum S/N. The line finder is therefore expected to preferentially find weaker systems in brighter quasars. A crucial step in our analysis will be to properly take this effect into account when we define a reference population of quasars without absorbers.

3.3.2. The simulated MgII samples

In order to test the efficiency of our detection technique and to identify biases and systematic effects we ran Monte Carlo simulations of the absorber catalog to create a sample of simulated MgII absorption lines reproducing the same properties as the real sample (z , W_0 , ΔW_0 , etc.) and same biases, but with the difference that the absorption lines are put in random spectra, i.e. that no correlation exists between quasar magnitude and absorber properties. Such a population can then be used as a control sample.

In order to create this sample, we proceed as follows: for each detected system, a simulated doublet having the same redshift, and similar $W_0(2796)$, doublet ratio, and Gaussian-fit width was put into many randomly selected EDR spectra. Each spectrum containing a simulated doublet was then run through the entire non-interactive

and interactive pipelines, and z and $W_0(2796)$ were measured for detected systems. Over 9100 simulated doublets were put in random quasar spectra. A large fraction of them appear in regions of spectra with insufficient signal to noise ratio to meet the detection threshold for the input $W_0(2796)$. The line finder is then able to recover about 4400 systems. Measurement error of the rest equivalent width $W_0(2796)$ can cause systems with $W_0(2796) < W_{lim}$ to scatter into the output catalog as well as systems with $W_0(2796) > W_{lim}$ to scatter out. Therefore, the recovered distribution of rest equivalent width differs from the input one. In order to create a simulated absorption line sample with statistically identical distributions of rest equivalent widths, a trial $W_0(2796)$ distribution was specified and then adjusted so that the simulated output best represents the data. We initially chose lines randomly from the input catalog according to a distribution of the form $N(W_0(2796)) \propto \exp^{-\frac{W_0}{W_{in}}}$ with an initial guess for W_{in} , until the number of lines recovered were equal to that of the actual catalog. Lines with input $W_0(2796) < 0.3$ Å were used, although only lines with recovered $W_0(2796) > 0.3$ Å were retained. We determined a maximum-likelihood value for W_{out} using the recovered $W_0(2796)$ values. We then corrected our guess for W_{in} to minimize $|W_{out} - W_{data}|$.

This procedure allows us to create a simulated absorption line sample having the same properties as the real sample described in the previous section. The distributions of real and simulated absorber redshifts, rest equivalent widths and rest equivalent widths uncertainties are presented in Fig 5. As can be seen, the statistical properties of the simulated samples match very well those of the real data. The figure shows that weaker absorption lines are preferentially found in high spectrum S/N – and therefore brighter quasars – in the same way as the real systems are. This bias is systematically introduced by the requirements of the line finder algorithm. Below we show that the selection of reference quasars described in the previous section takes this effect into account.

3.4. Defining reference quasars

As our goal is to isolate the magnitude shifts induced by intervening absorber systems, the selection of refer-

ence quasars must (i) not depend on quasar magnitudes and (ii) take into account the fact that the absorption line detectability depends on the spectrum S/N as seen above.

Here we describe how we define such populations of quasars: we first select the quasars with detected absorbers above a given rest equivalent width $W_0^{\lambda 2796} > 0.8 \text{ \AA}$. We will compare them to quasars without any detected absorber above this limit. In the goal of avoiding biases that would give rise to magnitude shifts, a number of criteria must be applied: the two quasar populations must have the same redshift distribution and present the same absorption-line detectability. For a given absorber with rest equivalent width W_0 and redshift z_{abs} , we randomly look for a quasar without any detected absorber (above $W_0^{\lambda 2796} = 0.8 \text{ \AA}$) such that:

(i) they have similar redshifts, i.e. $z_{QSOref} = z_{QSOabs} \pm 0.1$;

(ii) in addition, we need to check whether this quasar would have allowed for the detection of the absorption line, i.e. if its S/N at the corresponding wavelengths is high enough. Such a requirement translates into $W_{min}(QSO_{ref}, z_{abs}) < W_0$, where W_{min} is the minimum equivalent width that can be detected by the line finder at the corresponding wavelength. The quasars selected in this way are called *reference* quasars in the following. Our selection procedure ensures that if similar absorbers population were present in front of the selected reference quasars, we would have been able to detect them.

Since the number of available quasars without detected absorbers is larger than the number of quasars with absorbers for the range of W_0 we are interested in, we repeat the previous step N_b times in order to create a series of N_b reference samples that will be used for estimating the noise associated to a single quasar sample.

4. ANALYSIS & RESULTS

In order to isolate the magnitude changes due to the presence of the absorber systems we measure, in a given band j , the mean magnitude difference between quasars with absorbers and reference quasars:

$$\Delta \langle m_j \rangle = \langle m_{abs,j} \rangle - \langle m_{ref,j} \rangle . \quad (10)$$

As explained above, we can repeat the selection of reference quasars N_b times and create a series of reference samples in a bootstrap manner. The intrinsic dispersion of the series samples can then be used in order to estimate the errors in the measured magnitude shifts. As an example, we show in Figure 6 the results obtained by using a sample of quasars with MgII absorbers having $1.4 < W_0 < 2 \text{ \AA}$ and their corresponding reference quasars. The left panels show the magnitude distributions of quasars with absorbers (solid line histograms) and reference quasars (filled histograms). Within the Poisson noise, no significant difference can be seen between the two types of distributions. In the right panels, we show the mean magnitudes of these two populations. For each band, the vertical line shows the value $\langle m_{abs} \rangle$ and the histogram shows the distribution of the mean magnitudes $\langle m_{ref} \rangle$ of $N_b = 100$ reference samples. Such an estimator allows to reveal a significant difference between the magnitude distributions of the two populations and indicates that quasars with absorbers are affected by

reddening effects.

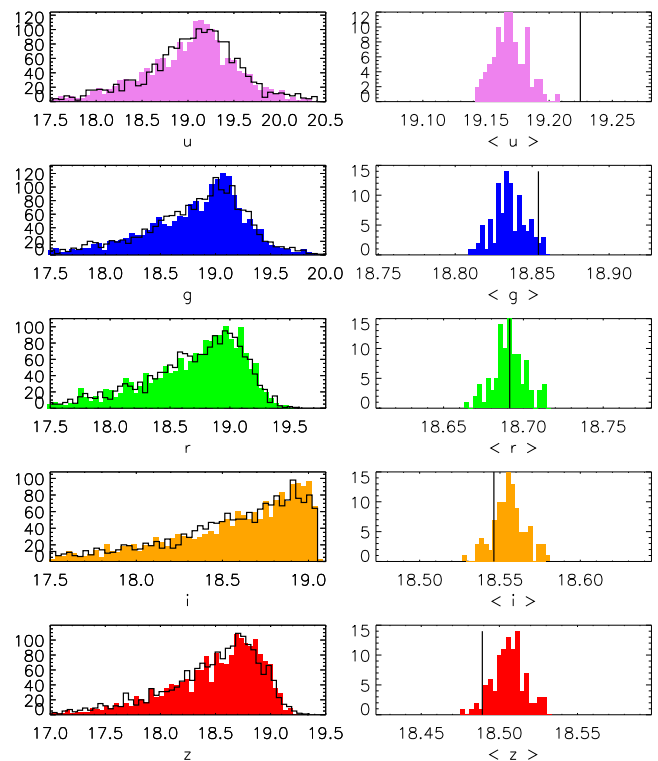


FIG. 6.— The left panels show the magnitude distributions of quasars with absorbers (solid line histograms) and reference quasars (filled histograms). Within the Poisson noise, no significant difference can be seen between the two types of distributions. In the right panels, we show the mean magnitudes of these two populations. For each band, the vertical line shows the value $\langle m_{abs} \rangle$ and the histogram shows the distribution of the mean magnitudes $\langle m_{ref} \rangle$ of N_b reference samples.

Before attempting to detect various signals with the data, we make use of the sample of simulated absorbers in order to test whether our procedure introduces any selection bias. Indeed, as measuring the quantity $\Delta \langle m_j \rangle$ involves the use of various procedures performed over a large number of objects (continuum normalization, line detectability, rest equivalent width fitting, etc.), it is important to investigate the presence of systematic effects and quantify them.

To check whether the properties of quasars with (detected) random absorption lines match those of quasars without, we proceed as follows: for a given sample of simulated absorbers, we define a population of reference quasars as defined in section 3.4. We then compare the mean magnitude difference between the two populations. Since the simulated absorption lines were initially put in random spectra, any departure from zero will quantify the level of systematics associated to our selection procedure. Such a process can therefore test whether the samples of quasars with and without absorption lines to have the statistical properties. We measure the corresponding mean magnitudes and the results are summarized in the left panel of Figure 7.

As can be seen, the mean magnitudes of these two samples are similar, but a non-zero magnitude difference is found and does not seem to depend on absorber rest

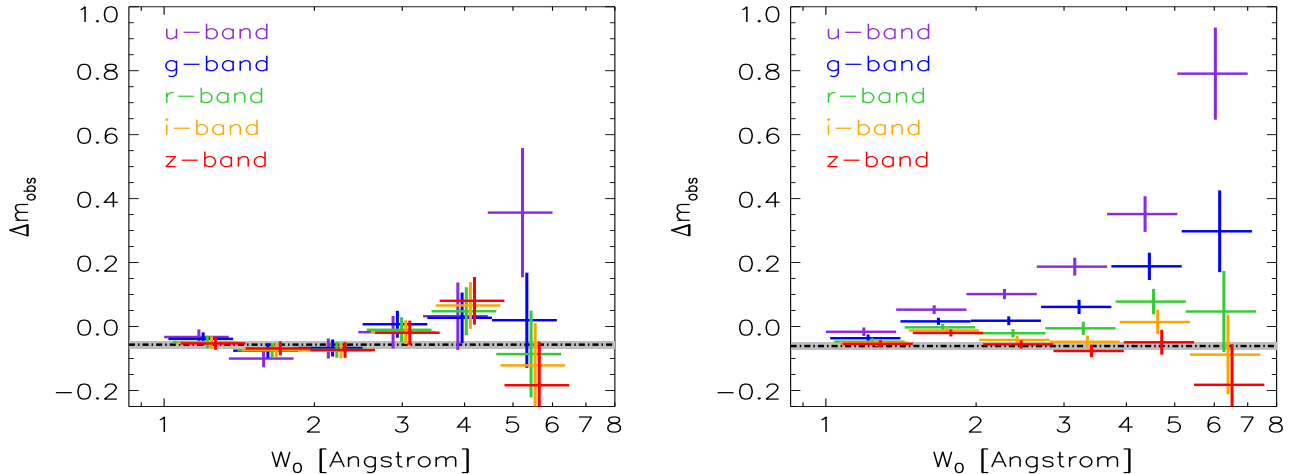


FIG. 7.— Mean magnitude shifts induced by the presence of absorber systems, as a function of rest equivalent width. *Left*: the results obtained using simulated absorption lines in random quasars show the existence of a bias giving rise to an excess brightening of $\Delta m \simeq 0.06$ (indicated by the gray region). *Right*: MgII absorbers detected in SDSS quasar spectra induced significant reddening and extinction effects. When the selection bias is taken into account, no significant quasar brightening can be observed.

equivalent width or wavelength. Using the z -band as a reference (the least affected by extinction effects, see section 4.1.5), the mean offset is found to be

$$\Delta\langle m \rangle_{bias} = -0.06 \pm 0.01 \text{ mag}. \quad (11)$$

Other bands give similar results, ranging from -0.05 ± 0.01 to -0.06 ± 0.01 . This negative value indicates that our global procedure, i.e. line finder and/or reference quasar selection, preferentially selects absorbers in brighter quasars. This systematic effect occurs at the 6% level in terms of quasar magnitude or similarly spectrum S/N. It could be corrected by increasing the estimates of W_{lim} by a similar amount. Here we prefer to take this effect into account by considering the existence of an offset in the mean magnitude differences. It should also be pointed out that our procedure indicates that the selection of absorption lines does not introduce any color-dependent bias. Indeed, no significant excess can be detected by comparing the colors of quasars with simulated absorption lines to those of reference quasars.

We now apply the same procedure to the sample of real MgII absorbers. The results are presented in the right panel of Figure 7. The gray region shows the zero point offset, $\Delta\langle m \rangle_{bias}$, given by the Montecarlo simulations. As we can see, it appears very clearly that the presence of a MgII absorber reddens the light of background quasars and the stronger the absorber rest equivalent width, the redder the quasar. The direct measurements indicate that $\Delta\langle m \rangle < 0$ for the strongest systems. However, by taking into account the offset due to the selection bias $\Delta\langle m \rangle_{bias}$, no significant difference can be observed. This result contrasts with a number of previous studies claiming that absorber systems are preferentially found in the spectrum of brighter quasars. It suggests that previous claims of such correlations may have arisen due to selection biases. The current analysis shows that the use of Montecarlo simulations in order to test the recovery of random absorption lines is an important task to achieve

in order to quantify the amount of systematic effects. More details on the reddening and magnification effects are presented below.

4.1. Dust reddening

From the magnitude shifts measured in each band we measure the corresponding color excess induced by MgII systems. The measured color excess induced by the presence of absorbers provides us with constraints on the properties of the dust associated with these systems such as the size distribution of the dust particles and the related column densities.

It should be noted that the magnitude shifts measured in different bands (fig. 7) are correlated and the errors on the colors are in general significantly smaller than the errors on the magnitude shifts. We have therefore computed the color covariance matrix from bootstrap resampling and estimated the errors on the measured color changes. The results are presented in fig. 8 where we show the mean color excess measured for the four color combinations $u-g$, $g-r$, $r-i$ and $i-z$, as a function of absorber rest equivalent width. As can be seen, strong MgII absorbers induce, on average, reddening values ranging from $E(g-r)_{obs} \sim 0.02$ to ~ 0.3 , which correspond to similar $E(B-V)_{obs}$ values.

As the SMC extinction curve is known to describe, on average, the reddening properties of MgII absorbers (Khare et al. 2005; Ménard et al. 2005; York et al. 2006), we can write

$$\langle E(B-V) \rangle \simeq \langle N_H(z) k(z) \rangle \times [\xi(\lambda_B) - \xi(\lambda_V)] \quad (12)$$

where $N_H(z)$ is the hydrogen column density associated to a MgII system, $k(z)$ is the dust to gas ratio, and $\xi(\lambda)$ is the wavelength dependence of the extinction curve. This relation shows that investigating the color excess as a function of redshift allows us to constrain the mean product $\langle N_H(z) k(z) \rangle$. In Figure 8 we have plotted the SMC-based reddening values for a series of amplitudes

normalized by the SMC dust column density

$$\frac{N_d}{N_{d,SMC}} = \left(\frac{k}{k_{SMC}} \right) \left(\frac{N_H}{10^{20}} \right) \text{ cm}^{-2}, \quad (13)$$

where k is the dust-to-gas ratio and N_H is the hydrogen column density. Our calculation includes the redshift distribution of the corresponding absorbers in each bin. First, we can see the SMC-like dust provides a good fit to the measured reddening for most of the absorber systems. The dotted lines can be used to quantify the amount of dust among various strengths of MgII absorbers. They correspond to $N_d/N_{d,SMC} = 1, 3, 10, 30$ and show that the optical depth for extinction spans a factor ~ 30 for MgII systems in the range $W_0 = 1$ to 6 \AA .

If the dust-to-gas ratio of MgII absorbers is comparable of that of the SMC, it implies that the strongest MgII absorbers have, on average, hydrogen column densities of $N_H \sim 10^{21} \text{ cm}^{-2}$, i.e. correspond to the regime of damped Lyman- α systems. This result is in agreement with the hydrogen column densities of MgII-selected systems measured by Rao et al. (2005).

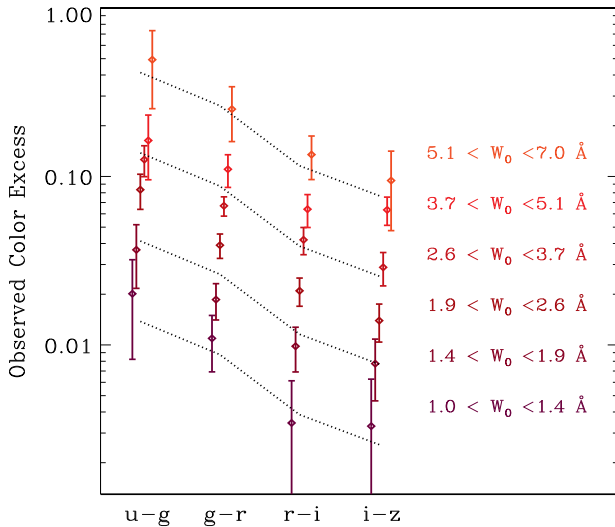


FIG. 8.— Color changes of quasars due to the presence of MgII absorbers, as a function of absorber rest equivalent width. The solid lines indicate the expected color changes due to an SMC reddening curve with different normalizations. The match between the slope of this curve and the data points show that the dust related to MgII systems is similar to SMC dust.

As the sensitivity of the SDSS filters is significantly lower in the u and z bands compared to the g, r and i ones, the $g-i$ color is measured the most accurately and will be used below to quantify reddening properties. We then convert the color excesses $E(g-i)$ into $E(B-V)$ and present the color excesses as a function of absorber rest equivalent width. The results are presented in Fig. 9. As can be seen, we find a strong correlation between these two parameters. We can also observe that the relation between observed mean $E(B-V)$ and W_0 is well described by a simple power-law:

$$\langle E(B-V)_{\text{obs}} \rangle (W_0) = C \left(\frac{W_0}{1 \text{ \AA}} \right)^\alpha, \quad (14)$$

with $C = (0.8 \pm 0.1) \times 10^{-2}$, $\alpha = 1.88 \pm 0.17$. As shown in section 2.1, for an SMC-type extinction law, the color excess $E(B-V)$ is roughly proportionally to the optical depth for extinction. Hence we can also write

$$\langle \tau_V \rangle (W_0) = \tau_{V,0} \left(\frac{W_0}{1 \text{ \AA}} \right)^\alpha, \quad (15)$$

with $\tau_{V,0} = (2.5 \pm 0.2) \times 10^{-2}$.

The relation holds for systems with $1 < W_0 < 7 \text{ \AA}$ which correspond to velocity dispersions spanning $100 \lesssim \Delta v \lesssim 700 \text{ km/s}$ and the dust column densities change by a factor ~ 30 in this range. The weakest and strongest absorbers of this sample are therefore significantly different but our results indicate that their dust and gas content follows a universal relation, suggesting that one phenomenon regulates, on average, the amount of one quantity with respect to the other. Modeling the gas distribution in the halo of galaxies is beyond the scope of this paper but we note that this relation strongly constrains theoretical models of absorber systems, as the dependence relates spatial information, τ_V , to a quantity that mostly carries velocity space information, W_0 . We believe that understanding this relation will greatly improve our knowledge about the nature of these systems.

If we consider the global distribution of strong MgII absorbers it is interesting to estimate the relative contribution of optical depth for extinction $\partial C_\tau / \partial W_0$, as a function of absorber rest equivalent width. Such a quantity is given by the product:

$$\frac{\partial C_{\tau_V}}{\partial W_0} = \frac{\partial N}{\partial W_0} \times \langle \tau_V \rangle (W_0). \quad (16)$$

The number of absorbers per unit rest equivalent width and redshift is given by Nestor et al. (2005):

$$\frac{\partial N}{\partial W_0} \lambda^{2796} = \frac{N^*}{W^*} e^{-\frac{W_0}{W^*}}, \quad (17)$$

with the maximum likelihood values $W^* = 0.702 \pm 0.017 \text{ \AA}$ and $N^* = 1.187 \pm 0.052$. This estimation takes into account incompleteness detections and is valid down to a rest equivalent width limit of $\sim 0.3 \text{ \AA}$. Using this result, we have computed the relative contribution of dust $\partial C_\tau / \partial W_0$, as a function of absorber rest equivalent width and present the results in the upper panel of Figure 9. The data points show that, for MgII systems with $W_0 > 1 \text{ \AA}$, most of the dust contribution originates from systems with $W_0 \sim 1 - 2 \text{ \AA}$. Therefore most of the extinction effects are expected to be associated to such systems. It is interesting to mention that an excess of MgII absorbers with $W_0 \simeq 2 \text{ \AA}$ is reported along gamma ray burst lines-of-sight with respect to those of quasars (Prochter et al. 2006).

We can also attempt to estimate the relative dust contribution originating from *all* MgII absorbers, i.e. including also weaker systems. First, we know that the functional form used for the incidence of MgII absorbers $\partial N / \partial W_0 \lambda^{2796}$ holds down to systems as weak as $\sim 0.3 \text{ \AA}$. In the range 0.3 to 1 \AA we do not have any detection of dust reddening but we can attempt to extrapolate the scaling found above (eq. 16). By doing so, we find

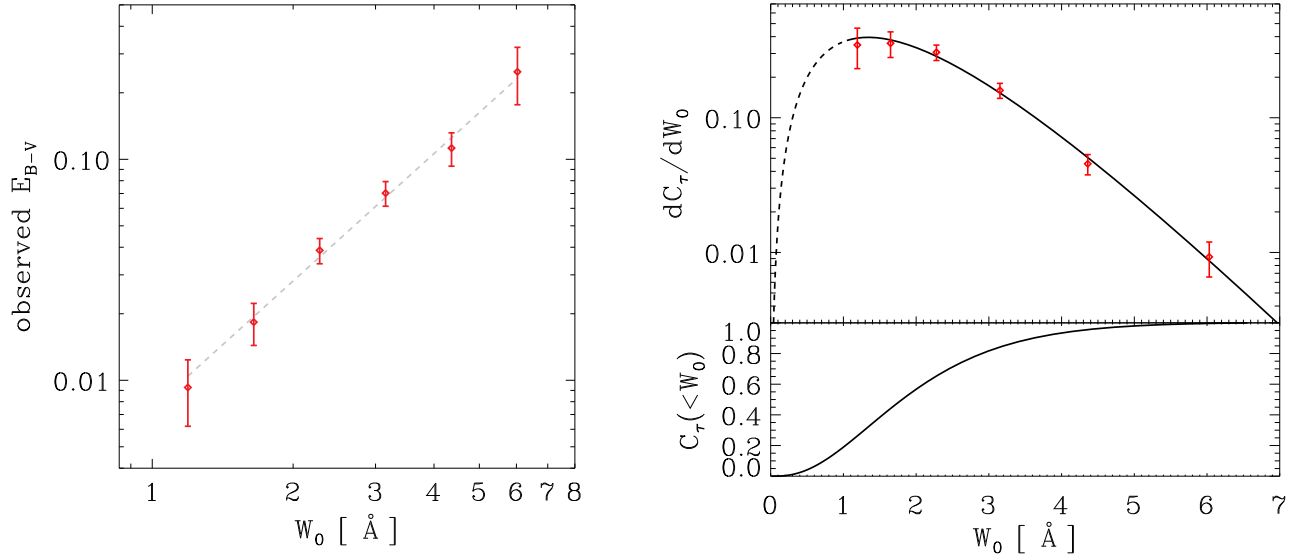


FIG. 9.— *Left*: Mean $E(B-V)$ values observed as a function of absorber rest equivalent width W_0 . A power-law fit gives: $\langle E(B-V) \rangle = (0.008 \pm 0.001) \times W_0^{1.88 \pm 0.17}$. *Right, top panel*: the relative contribution of mean dust column density, $\partial C_\tau / \partial W_0$, as a function of MgII rest equivalent width. The dashed line shows the behavior obtained by extrapolating the observed relation between $E(B-V)$ and W_0 . Using such an assumption, we show the cumulative distribution of dust column density $C(<W_0)$ in the bottom panel. Most of the dust is expected to be carried by MgII systems with $W_0 > 1 \text{ \AA}$.

that the global dust contribution originating from systems weaker than 1 \AA is smaller than $\sim 20\%$. The result is similar if, instead of extrapolating eq. 16, we use an upper limit from systems with $W_0 \simeq 1 \text{ \AA}$, i.e. the weakest systems used in the present analysis. Therefore, *the vast majority of the dust probed by MgII absorption lines originates from strong systems, with $W_0 > 1 \text{ \AA}$* . As dust originates from stars, this result appears to be in line with the association between strong MgII absorbers and $\sim L_*$ galaxies, i.e. galaxies from which most of the star light originates.

4.1.1. Dust redshift evolution

We now investigate the dust column densities associated with MgII systems as a function of redshift. Using an SMC-type extinction curve, we have computed the rest frame $E(B-V)$ values as a function of rest equivalent width for three redshift bins. The results are presented in Figure 10 and show that the scaling between $E(B-V)$ and W_0 found in the previous section is consistent with being redshift independent but the overall amplitude decreases with redshift indicating that MgII absorbers are less dusty at earlier times.

In order to quantify the redshift evolution of the dust, we measure the average $E(B-V)$ of all absorbers systems with $W_0 > 1 \text{ \AA}$, in three redshift bins spanning the range $0.4 < z < 2.2$. In each case we measure the observed and rest frame $E(B-V)$ values. The results are shown in the right panel of Figure 10. As we can see, the observed reddening effects of MgII systems are on average consistent with being redshift independent. Our vision of the distant universe is equally affected by MgII absorbers at $z \sim 0$ and $z \sim 2$. In contrast, the *rest frame* $E(B-V)$ values, and therefore the dust column densities, show a significant redshift evolution. We find

that the amount of dust associated with MgII absorbers increases by more than a factor two between $z = 2$ and $z = 0.4$. A simple power law fit to the data points gives $E(B-V)_{rest} \propto (1+z)^{-1.1 \pm 0.4}$.

It is interesting to see that such a variation is similar to that of the cosmic star density Ω_* . We illustrate this agreement in the figure by showing the integrated star formation rate given by Hernquist & Springel (2003) where the scaling has been renormalized to the reddening values. Our results therefore provide a new and independent method to probe the star formation rate over cosmological time scales.

If we assume that the redshift and rest equivalent widths dependencies can be separated (as suggested by the data points), we can write that

$$\langle E(B-V)_{rest} \rangle (W_0, z) = C' \times \left(\frac{W_0}{1 \text{ \AA}} \right)^\alpha (1+z)^\beta, \quad (18)$$

where $\alpha = 1.88 \pm 0.17$ (see section 4.1), $\beta = -1.1 \pm 0.4$ and $C' = (0.60 \pm 0.07) \times 10^{-2}$. This functional form provides us with interesting constraints on the properties of cold gas and dust. It will be particularly interesting to include such information in theoretical models of absorber systems.

4.1.2. Dust-to-metals ratio

We can use the above results to estimate the dust-to-metals ratio of MgII absorbers by computing the ratio

$$\mathcal{R}_{DM} \equiv \langle E(B-V) \rangle / \langle N(ZnII) \rangle, \quad (19)$$

adopting Zn (an undepleted Fe-peak element) as an indicator of overall metal content. This ratio provides us with an estimate of the fraction of refractory elements depleted onto dust grains, a quantity determined

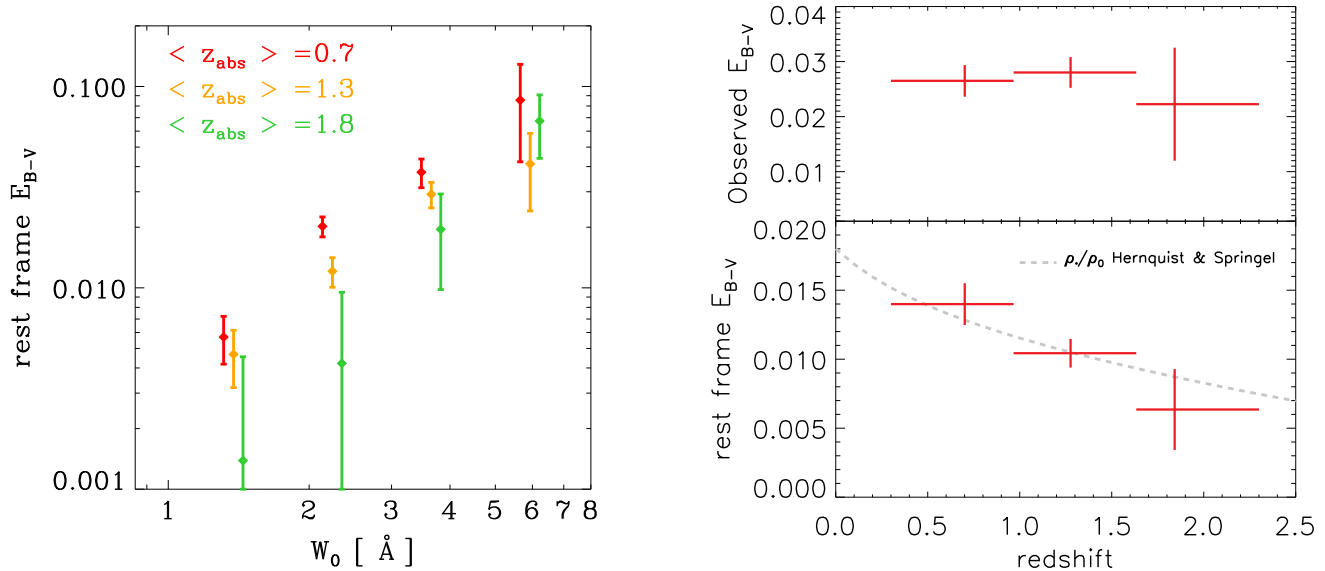


FIG. 10.— *Left*: Rest frame E(B-V) induced by MgII absorbers measured for three redshift bins, and as a function of MgII rest equivalent width. *Right*: Evolution of the global E(B-V) (for all MgII systems with $W_0 > 1$ Å) as a function of redshift. This trend shows that the mean product $\langle N_H(z)k(z) \rangle$ increases by a factor ~ 2 between $z = 2$ and $z = 0.5$. This is comparable to the evolution of the cosmic star density (or integrated star formation rate) illustrated here by the (renormalized) model by Hernquist and Springel (2005).

by the balance between the formation and destruction of dust particles. Using a similar sample of MgII absorbers with $z \sim 1$, Nestor et al. (2003) have measured the mean rest equivalent width of $ZnII\lambda 2026$ and found $W_0 = 0.033 \pm 0.005$ Å. Assuming that most of the zinc is in the form of ZnII, we obtain $N_{Zn} = (3.63 \pm 0.5) \times 10^{12}$ cm $^{-2}$. Combining this value with our estimate of the mean E(B-V) of MgII systems at $z \sim 1$ we find

$$\mathcal{R}_{\text{DM}} = (4.1 \pm 0.6) \times 10^{-15} \text{ mag cm}^2. \quad (20)$$

As shown by Wild et al. (2006, see their table 5), the dust-to-metals ratios, \mathcal{R}_{DM} , of the Milky way, LMC and SMC are 4.7, 3.1 and 1.6×10^{-15} mag cm 2 , respectively. Our analysis therefore shows that, on average, MgII absorbers with $W_0 > 1$ Å have a dust-to-metals ratio similar to that of our Galaxy. The properties of \mathcal{R}_{DM} as a function of redshift and MgII rest equivalent width will be presented in a future paper.

4.1.3. Dust extinction bias in magnitude limited QSO samples

From the observed E(B-V) values, we can now use the results of the reddening MonteCarlo simulations presented in section 3.2 and infer the fraction of quasars with absorbers missed in the magnitude limited sample. Note that our procedure takes into account quasars missed due to both magnitude and color selections. Assuming that the distribution of intrinsic reddening values is not strongly skewed (which is suggested by the results of Ellison et al. (2004) with radio-selected quasars), we estimate the fraction of MgII absorbers missed due to extinction effects and present the results in Fig. 11. The fraction of missed systems is below one percent for absorbers with $W_0 \simeq 1$ Å. However, above this value, incompleteness effects become more important. Our analysis indicates that the SDSS misses more than 10% of

$W_0 \sim 3$ Å MgII absorbers and this rises to more than 50% at $W_0 \sim 6$ Å. By extrapolating the trend to stronger systems, we see that the SDSS could not detect MgII systems with $W_0 \gtrsim 10$ Å. The fraction of missed quasars with absorbers can be parametrized by

$$\langle f_m \rangle (W_0) = C_m \left(\frac{W_0}{1 \text{ Å}} \right)^\gamma, \quad (21)$$

with $C_m = 0.005 \pm 0.001$ and $\gamma = 2.23 \pm 0.18$.

The knowledge of f_m allows us to estimate the global fraction of quasars with strong MgII absorbers, *per unit redshift*, missed due to the extinction bias. We have

$$\begin{aligned} f_m^{\text{tot}} &= \int_1^\infty f_m(W_0) \frac{\partial N}{\partial W_0} W_0 \\ &\simeq \int_0^\infty f_m(W_0) \frac{\partial N}{\partial W_0} W_0 \\ &\simeq 0.01 \end{aligned} \quad (22)$$

Therefore, if we consider quasars at $z = 1$, about one percent of them cannot be observed due to extinction effects by MgII systems. As both $\partial N/\partial W_0$ and the observed $E(B-V)$ of MgII systems do not vary strongly with redshift (see section 4.1.1), this missing fraction is roughly proportional to the quasar redshift. Therefore, if we consider the main sample of SDSS quasars (for which the mean redshift is above 1.5) the incompleteness due to the dust hosted by MgII absorbers is about 2%.

4.1.4. Recovering the unbiased $\partial N/\partial W_0$ distribution

As the fraction of missed quasars with absorbers depends on W_0 , the observed distribution of absorber rest equivalent widths differs from the intrinsic one and we

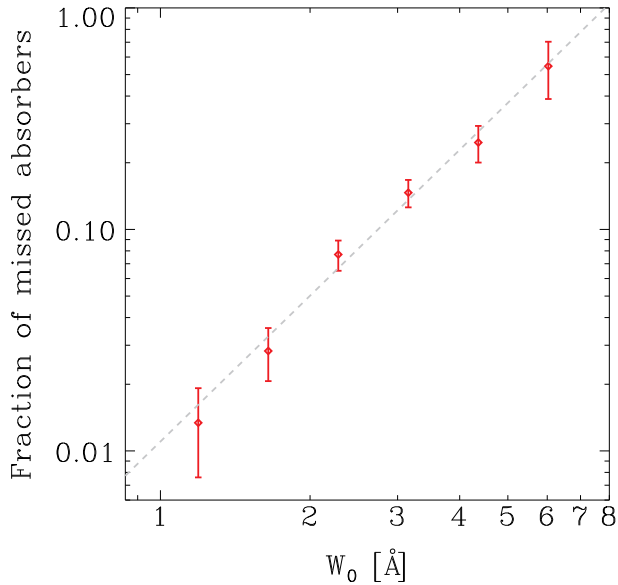


FIG. 11.— Fraction of quasars with MgII systems that is observed due to reddening and extinction effects. For the strongest systems we can see that almost half of the objects are missed in this magnitude limited sample.

have

$$\left(\frac{\partial N}{\partial W_0}\right)_{int} = \left(\frac{\partial N}{\partial W_0}\right)_{obs} \frac{1}{1 - f_m(W_0)}. \quad (23)$$

As we have used the functional form of $\partial N/\partial W_0$ to estimate the missing fraction f_m , an exact estimation of these quantities should be made with an iterative process using eq. 23. However, given the small values of f_m and the exponential cutoff of $\partial N/\partial W_0$, such an approach will only bring negligible corrections to f_m . Our previous estimations are therefore robust.

The values of f_m shown in Figure 11 indicate that the shape of the observed distribution of $\partial N/\partial W_0$ is expected to be significantly affected at the high-end values and to present a deficit.

4.1.5. Gravitational lensing

In order to detect the potential effects of gravitational lensing, we now estimate the magnitude shifts induced by the presence of strong MgII absorbers, after correcting for dust extinction.

In section 3.2 we have shown that, on average, the induced and measured color excess are equivalent (in the range of values of interest in our analysis). However, given the shape of the QSO magnitude distribution and the selection criteria of the SDSS quasar target algorithm, a difference exists between induced and measured extinction. Having quantified these effects in section 3.2, we can now use the observed $E(B - V)$ values and apply the appropriate *observed* extinction correction to the quasar magnitudes. The corresponding results are shown in Fig. 12 where the horizontal line represents the zero point obtained with the Monte Carlo simulations for simulated absorption lines. By comparing the extinction-corrected magnitude shifts to this reference level, we do

not find any significant magnification signal (for which Δm would be negative).

If we consider all strong MgII absorbers with $W_0 > 1 \text{ \AA}$, we find the mean magnitude shift in the z band to be:

$$\begin{aligned} \langle \Delta u \rangle &= 0.028 \pm 0.015 \\ \langle \Delta g \rangle &= 0.015 \pm 0.014 \\ \langle \Delta r \rangle &= 0.015 \pm 0.013 \\ \langle \Delta i \rangle &= 0.015 \pm 0.013 \\ \langle \Delta z \rangle &= 0.010 \pm 0.013 \end{aligned} \quad (24)$$

which was compared to the zero-point and taking into account its uncertainty. These mean magnitude shifts are consistent with zero ($\langle \Delta u \rangle$ is positive at the $2\text{-}\sigma$ level only). Our analysis does not show any detectable brightening effect, which differs from a number of previous studies claiming detections of magnification effects due to metal absorbers. It is interesting to point out that without the quantification of systematic effects done with the Monte Carlo simulations, i.e. without the calibration of the zero point, the raw measurement with the real data would have led to the detection of a negative magnitude shift which could have been interpreted as magnification effects.

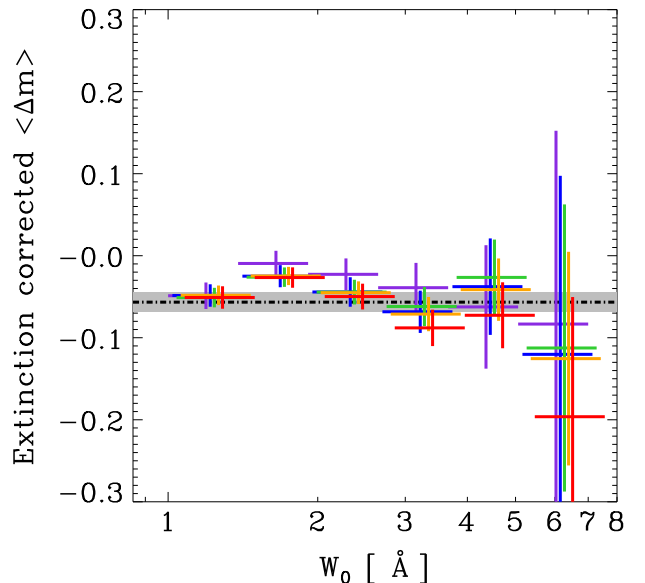


FIG. 12.— Mean QSO magnitude shift due the presence of a strong MgII absorber, after correcting for dust extinction, as a function of absorber rest equivalent width W_0 . The horizontal line represents the zero point calibrated with Monte Carlo simulations using simulated absorption lines in real SDSS quasar spectra. The colors denote the filter names (see Fig. 7). Our analysis does not show any significant magnification effect, which would correspond to a negative $\langle \Delta m \rangle$.

We can use the above results to infer an upper limit on magnification effects. If we consider the g, r and i bands the $3\text{-}\sigma$ upper limit on magnification is

$$\langle \Delta m \rangle_{lensing} \simeq -0.024. \quad (25)$$

As explained in section 4.1.5 and detailed in Ménard (2005), given the shape of the quasar magnitude distribution, this corresponds to an upper limit for the mean magnification:

$$\langle \mu \rangle \lesssim 1.10, \quad (26)$$

meaning that the excess magnification is smaller than about ten percent. In order to convert this value into a more interesting quantity, we can assume the mass distribution of the galaxies responsible for the absorption to follow that of a singular isothermal sphere. The galactic halos therefore have the following density and surface density:

$$\rho \propto \frac{\sigma_v^2}{r^2} \quad \text{and} \quad \Sigma(r) = \frac{\sigma_v^2}{2Gr}, \quad (27)$$

and the corresponding magnification effects of a point source can then be computed in a simple way:

$$\mu = \begin{cases} 2/y & \text{if } y \leq 1 \\ 1 + 1/y & \text{if } y \geq 1 \end{cases} \quad (28)$$

where y is the impact parameter normalized to the Einstein radius of the lens:

$$\zeta_0 \equiv 4\pi \left(\frac{\sigma_v}{c} \right)^2 \frac{D_d D_{ds}}{D_s}, \quad (29)$$

where σ_v is the velocity dispersion and $D_{d,s,ds}$ are the angular diameter distances from the observer to the lens, to the source, and from the lens to the source. Using the above upper limit on the magnification, and the average impact parameter for MgII systems with $W_0 > 1 \text{ \AA}$ recently measured by Zibetti et al. (2006): $\langle b \rangle \simeq 40 \text{ kpc}$, we find

$$\sigma_v \lesssim 269 \text{ km s}^{-1}, \quad (30)$$

for absorbers at $z = 0.5$ and quasars at $z = 1$. This result shows that, on average, MgII absorbers are not associated with massive elliptical galaxies and is in agreement with previous estimates based on different methods. Previous works have shown that the average MgII absorbing galaxy has a luminosity about $\simeq 0.8 L_*$ (Zibetti et al. 2007; Steidel et al. 1997). The expected velocity dispersion of the gravitational potential of such galaxies is expected to be $\sim 150 \text{ km s}^{-1}$. Therefore the sensitivity of the present measurement needs to be improved only by a factor of a few in order to detect the magnification signal originating from the galaxies associated with MgII absorbers. The present analysis is based only on quasars with $i < 19.1$. In the future, it might be of interest to quantify the selection effects of fainter SDSS quasars as it would double the sample size. In a longer term, being able to measure this magnification signal as a function of absorber rest equivalent width and redshift will provide us with important constraints on the nature and environment of metal absorbers.

5. SUMMARY

We have used a sample of almost 7000 strong MgII absorbers with $0.4 < z < 2.2$ detected in the SDSS DR4 dataset to investigate the gravitational lensing and dust reddening effects they induce on background quasars. We have attempted to make significant improvements in making such measurements, by using a sample of MgII

absorbers an order of magnitude larger than earlier analyzes and by carefully quantifying a number of systematic effects previously neglected.

In order to do so we have restricted our analysis to a well defined sample of $\sim 30,000$ SDSS quasars with $i < 19.1$ and considered strong MgII absorbers with a rest equivalent width $W_0 > 1 \text{ \AA}$. We have quantified the efficiency of the absorption-line finder algorithm with Monte Carlo simulations and the sensitivity of the SDSS quasar target algorithm to detect reddened quasars. We then measured the statistical magnitude changes induced by the presence of MgII absorbers.

Our main results are as follows:

(i) Strong MgII absorbers significantly redden the light of their background quasars. We confirm previous results showing that, on average, the dust particle size distribution of these systems is similar to that of the SMC, i.e. without the presence of a reddening excess at $0.2 \mu\text{m}$. Moreover, we find that the *observable* reddening effects follow the simple relation: $\langle E(B - V)_{\text{obs}} \rangle (W_0) = C (W_0)^\alpha$, with $C = (0.8 \pm 0.1) \times 10^{-2}$, $\alpha = 1.88 \pm 0.17$, for absorbers with $1 < W_0 < 6 \text{ \AA}$. In this range, the mean dust column density increases by a factor ~ 30 . Since most MgII lines with $W_0 > 1 \text{ \AA}$ are saturated, this scaling suggests that, on average, the dust column density is proportional to the velocity dispersion of the gas. Such a relation provides us with an important constraint for theoretical models of absorber systems.

(ii) The analysis of reddening effects as a function of has shown that the *rest-frame* $E(B - V)$ values follows $\langle E(B - V) \rangle \propto (1+z)^{-\beta}$, with $\beta = 1.1 \pm 0.4$, which implies that the amount of dust in MgII systems increases by a factor ~ 2 between $z = 2$ and $z = 0.5$. Such a trend is similar to the evolution of the cosmic star density. Our results therefore provide a new and independent method to probe the star formation rate through the production of dust over cosmological time scales.

The *observed* $E(B - V)$ values induced by MgII appear to be consistent with no redshift evolution down to $z = 2$. This observation results from less dust at higher redshift being canceled out by higher SMC extinction at high redshift (which probe bluer rest-frame wavelengths). We have also showed that, considering all MgII absorbers, most of the dust is carried by systems with $W_0 \sim 1 - 2 \text{ \AA}$.

(iii) We have estimated the dust-to-metals ratio of MgII absorbers by measuring the quantity $\mathcal{R}_{\text{DM}} \equiv \langle E(B - V) \rangle / \langle N_{\text{Zn}} \rangle = (4.1 \pm 0.6) \times 10^{-15} \text{ mag cm}^2$ which is similar to that of the Milky way.

(iv) We have quantified the fraction of absorbers and/or quasars missed due to extinction effects induced by MgII systems. While less than 2% of absorbers with $W_0 \sim 1 \text{ \AA}$ are missed, this fraction increases up to $\sim 30\%$ for the strongest systems of our sample, with $W_0 \sim 6 \text{ \AA}$. This effect therefore affects the shape of the distribution of absorber rest equivalent widths and we provide a correction factor for it. We also show that extinction effects due to MgII systems decrease the number of observable quasars by less than 2%.

(v) Regarding gravitational lensing, in contrast to previous studies we do not find an excess of absorbers in brighter quasars and we obtain only an upper limit on gravitational magnification: $\mu(W_0^{2796} > 1 \text{ \AA}) < 1.10$. We have shown that testing the global selection procedure (for detecting absorption lines and defining reference quasars) is crucial in order to make such a measurement. Our result provides an upper limit for the velocity dispersion of MgII absorbing galaxies: $\sigma_v \lesssim 269 \text{ km s}^{-1}$. As it has been shown that the mean luminosity of MgII absorbing galaxies is about $\sim 0.8 L_*$ (Zibetti et al. 2007), it implies that improving the sensitivity of our measurements by a factor of a few might lead to the detection of the magnification effects induced by MgII absorbing galaxies and therefore a characterization of their mass.

6. FUTURE DIRECTIONS

Understanding the nature of the structures probed by absorption lines is an important task to be achieved. Among metal lines, the MgII doublet, $\lambda\lambda 2796, 2803 \text{ \AA}$ is one of the most commonly detected features in optical quasar spectra but little is known about the properties and origin of MgII absorber systems. Attempts to find correlations between W_0 and galaxy parameters have turned out to be rather difficult. Recently, using HST images of 37

galaxies giving rise to MgII absorption, Kacprzak et al. (2007) showed that most galactic parameters do *not* correlate with absorption strength.

In this paper we have shown the existence of a well-defined scaling relation between the mean E(B-V) induced by MgII absorbers and their rest equivalent width W_0 , and presented its evolution as a function of redshift. Since most MgII lines with $W_0 > 1 \text{ \AA}$ are saturated, this scaling translates into a relation between dust column density and gas velocity dispersion, with Δv spanning the range 100 to about 600 km/s. Theoretical models are needed in order to gain insight into the origin of this relation. We believe that being able to understand and reproduce this scaling will shed light on the nature and properties of the structures traced by low-ionization absorption lines.

ACKNOWLEDGMENTS

B. M. thanks Nadia Zakamska for her help with using the SDSS pipeline. Funding for the creation and distribution of the SDSS Archive has been provided by the Alfred P. Sloan Foundation, the Participating Institutions, the National Aeronautics and Space Administration, the National Science Foundation, the U.S. Department of Energy, the Japanese Monbukagakusho, and the Max Planck Society.

REFERENCES

- Bartelmann, M., & Loeb, A. 1996, ApJ, 457, 529
 Bartelmann, M., & Loeb, A. 1998, ApJ, 503, 48
 Bergeron, J., & Boisse, P. 1991, A&A, 243, 344
 Bergeron, J., Cristiani, S., & Shaver, P. A. 1992, A&A, 257, 417
 Borgeest, U., & Mehlert, D. 1993, A&A, 275, L21
 Bouché, N., Murphy, M. T., Péroux, C., Csabai, I., & Wild, V. 2006, MNRAS, 371, 495
 Bowen, D. V., et al. 2006, ApJ, 645, L105
 Bowen, D. V., Chelouche, D., Ménard, B., in preparation
 Chelouche, D., Ménard, B., Bowen, D. V., Gnat, O., in preparation
 Churchill, C. W., Mellon, R. R., Charlton, J. C., Jannuzi, B. T., Kirhakos, S., Steidel, C. C., & Schneider, D. P. 2000, ApJS, 130, 91
 Churchill, C. W., Kacprzak, G. G., & Steidel, C. C. 2005, Proceedings of the IAU Colloquium 199 "Probing Galaxies through Quasar Absorption Lines", arXiv:astro-ph/0504392
 Ellison, S. L., Churchill, C. W., Rix, S. A., & Pettini, M. 2004, ApJ, 615, 118
 Ellison, S. L., Hall, P. B., & Lira, P. 2005, AJ, 130, 1345
 Hernquist, L., & Springel, V. 2003, MNRAS, 341, 1253
 Hopkins, P. F., et al. 2004, AJ, 128, 1112
 Kacprzak, G. G., Churchill, C. W., Steidel, C. C., Murphy, M. T., & Evans, J. L. 2007, ArXiv Astrophysics e-prints, arXiv:astro-ph/0703377
 P. Khare, D. G. York, D. Vanden Berk, V. P. Kulkarni, A. P. S. Crotts, D. E. Welty, J. T. Lauroesch, G. T. Richards, Y. Alsayyad, A. Kumar, B. Lundgren, N. Shanidze, J. Vanlandingham, B. Baugher, P. B. Hall, E. B. Jenkins, B. Ménard, S. Rao, D. Turnshek, C. W. Yip, Proceedings of the IAU Colloquium 199 "Probing Galaxies through Quasar Absorption Lines", astro-ph/0504532
 Lanzetta, K. M., Wolfe, A. M., & Turnshek, D. A. 1987, ApJ, 322, 739
 Le Brun V., Bergeron J., Boisse P., Christian C., 1993, A&A, 279, 33
 Ménard, B. 2005, ApJ, 630, 28
 Ménard, B., Zibetti, S., Nestor, D., & Turnshek, D. 2005, IAU Colloq. 199: Probing Galaxies through Quasar Absorption Lines, 86
 Ménard, B. and Péroux, C., A&A 410, 43
 Nestor, D. B., Rao, S. M., Turnshek, D. A., & Vanden Berk, D. 2003, ApJ, 595, L5
 Nestor, D. B., Turnshek, D. A., & Rao, S. M. 2005, ApJ, 628, 637
 Pei, Y. C., Fall, S. M., & Bechtold, J. 1991, ApJ, 378, 6
 Pei, Y. C. 1992, ApJ, 395, 130
 Perna, R., Loeb, A., & Bartelmann, M. 1997, ApJ, 488, 550
 Prevot, M. L., Lequeux, J., Prevot, L., Maurice, E., & Rocca-Volmerange, B. 1984, A&A, 132, 389
 Prochaska, J. X., Herbert-Fort, S., & Wolfe, A. M. 2005, ApJ, 635, 123
 Prochter, G. E., Prochaska, J. X., & Burles, S. M. 2006, ApJ, 639, 766
 Rao, S. M., Turnshek, D. A., & Nestor, D. B. 2006, ApJ, 636, 610
 Richards, G. T., York, D. G., Yanny, B., Kollgaard, R. I., Laurent-Muehleisen, S. A., & vanden Berk, D. E. 1999, ApJ, 513, 576
 Richards, G. T., et al. 2001, AJ, 121, 2308
 Richards, G. T., et al. 2002, AJ, 123, 2945
 Richards, G. T., et al. 2003, AJ, 126, 1131
 Richards, G. T., et al. 2005, MNRAS, 360, 839
 Richards, G. T., et al. 2006, ApJS, 166, 470
 Schneider, D. P., et al. 2002, AJ, 123, 567
 Smette, A., Claeskens, J., & Surdej, J. 1997, New Astronomy, 2, 53
 Steidel, C. C., & Sargent, W. L. W. 1992, ApJS, 80, 1
 Steidel, C. C., Dickinson, M., & Persson, S. E. 1994, ApJ, 437, L75
 Steidel, C. C., Dickinson, M., Meyer, D. M., Adelberger, K. L., & Sembach, K. R. 1997, ApJ, 480, 568
 Thomas, P. A., & Webster, R. L. 1990, ApJ, 349, 437
 Tripp, T. M., & Bowen, D. V. 2005, IAU Colloq. 199: Probing Galaxies through Quasar Absorption Lines, 5
 Turnshek, D. A., Lupie, O. L., Rao, S. M., Espey, B. R., & Sirola, C. J. 1997, ApJ, 485, 100
 vanden Berk, D. E., Quashnock, J. M., York, D. G., & Yanny, B. 1996, ApJ, 469, 78
 Vladilo, G., Centurión, M., Levshakov, S. A., Péroux, C., Khare, P., Kulkarni, V. P., & York, D. G. 2006, A&A, 454, 151
 Vladilo, G., & Péroux, C. 2005, A&A, 444, 461
 Wild, V., & Hewett, P. C. 2005, MNRAS, 361, L30
 Wild, V., Hewett, P. C., & Pettini, M. 2006, MNRAS, 367, 211
 York, D. G., Yanny, B., Crotts, A., Carilli, C., Garrison, E., & Matheson, L. 1991, MNRAS, 250, 24
 York, D. G., et al. 2000, AJ, 120, 1579
 York, D. G., et al. 2006, MNRAS, 367, 945
 Zibetti, S., Ménard, B., Nestor, D., & Turnshek, D. 2005, ApJ, 631, L105
 Zibetti, S., Ménard, B., Nestor, D. B., Quider, A. M., Rao, S. M., & Turnshek, D. A. 2007, ApJ, 658, 161